THE JOURNAL OF BIOLOGICAL CHEMISTRY VOL. 286, NO. 37, pp. 32251–32258, September 16, 2011

Evidence for an Extended Hydrogen Bond Network in the Binding Site of the Nicotinic Receptor

ROLE OF THE VICINAL DISULFIDE OF THE α1 SUBUNIT[*S]

Received for publication, April 25, 2011, and in revised form, July 8, 2011 Published, JBC Papers in Press, July 13, 2011, DOI 10.1074/jbc.M111.254235

Angela P. Blum[‡], Kristin Rule Gleitsman[‡], Henry A. Lester[§], and Dennis A. Dougherty[‡1]

From the Divisions of [‡]Chemistry and Chemical Engineering and [§]Biology, California Institute of Technology, Pasadena, California 91125

The defining feature of the α subunits of the family of nicotinic acetylcholine receptors is a vicinal disulfide between Cys-192 and Cys-193. Although this structure has played a pivotal role in a number of pioneering studies of nicotinic receptors, its functional role in native receptors remains uncertain. Using mutant cycle analysis and unnatural residue mutagenesis, including backbone mutagenesis of the peptide bond of the vicinal disulfide, we have established the presence of a network of hydrogen bonds that extends from that peptide NH, across a β turn to another backbone hydrogen bond, and then across the subunit interface to the side chain of a functionally important Asp residue in the non-α subunit. We propose that the role of the vicinal disulfide is to distort the β turn and thereby properly position a backbone NH for intersubunit hydrogen bonding to the key Asp.

Nicotinic acetylcholine receptors (nAChRs)[2] are neurotransmitter-gated ion channels that mediate rapid synaptic transmission throughout the central and peripheral nervous systems (1–3). The nAChR family members are also the prototypes of a large class of channels termed Cys-loop (or pentameric) receptors, which are essential for learning, memory, and sensory perception and are implicated in numerous neurological disorders, including Alzheimer disease, Parkinson disease, and schizophrenia (4, 5). Of the 17 genes that code for subunits of the nAChR, 10 produce α subunits. The α subunits of nAChRs typically contain the principal component of the agonist binding site and are distinguished by a unique vicinal disulfide at the agonist binding site formed by residues canonically labeled as Cys-192 and Cys-193. As shown in Fig. 1, the vicinal disulfide produces an eight-membered ring that contains an amide and a disulfide, two functionalities with distinct conformational properties.

In the 1960s, reduction of this disulfide in the *Electrophorus* electroplax led to the realization that the nAChR, long defined as controlling the ion conductance of the membrane, is a protein (6–8). That this disulfide can be more easily reduced than a typical protein disulfide was later rationalized by the finding that the disulfide is vicinal and therefore embedded in a strained ring (9, 10). The vicinal disulfide has been included and discussed in many classic studies in early nAChR research because of its susceptibility to reduction and proximity to the agonist binding site (6, 7, 11–16).

Nevertheless, the precise role of the vicinal disulfide in nAChR function is not established. Early studies (17) seemed to indicate that reduction of this disulfide rendered the receptor nonfunctional (but see below). Computational, NMR, and crystallographic studies of model vicinal disulfides have probed the multiple conformational possibilities of this unique structural unit (18–22). The *trans* conformation that is overwhelmingly preferred for backbone amides is expected to be disfavored in the context of an eight-membered ring, allowing for an energetically accessible *cis* backbone conformation. Also, a gauche conformation is strongly preferred about the S–S disulfide bond (C–S–S–C dihedral angle ~90°). In the context of the ring formed by the vicinal disulfide, the gauche(+) and gauche(−) forms produce energetically distinct (diastereomeric) structures. The combined backbone and disulfide conformational combinations give rise to four distinct conformers for the vicinal disulfide ring.

Although the sulfurs of the disulfide can contact small molecules that bind to the acetylcholine-binding protein (AChBP) (23, 24), a very useful model of the nAChR binding site, any noncovalent interactions of this sort are expected to be quite weak. Instead, many workers have speculated on a role in receptor gating involving *cis-trans* isomerization of the amide and/or gauche(+)/gauche(−) interconversion of the disulfide (10, 18, 19, 21, 22). Conventional mutagenesis studies are expected to produce severely impaired receptors, and so it has been challenging to design unambiguous probes of disulfide function.

Here we use subtle structural variations enabled by unnatural amino acid mutagenesis to evaluate the possible functional role of the vicinal disulfide of nAChR α subunits. We find evidence that the vicinal disulfide contributes to an interesting triad of residues that forms a network of hydrogen bonds that spans the interface between two subunits and impacts receptor function.

* This work was supported, in whole or in part, by National Institutes of Health Grants NS 34407 (to D. A. D.) and NS 11756 (to H. A. L.).

[S] The on-line version of this article (available at http://www.jbc.org) contains supplemental text and supplemental Table S1.

[1] To whom correspondence should be addressed: Division of Chemistry and Chemical Engineering, California Institute of Technology, 1200 E. California Blvd., Pasadena, CA 91125. Tel.: 626-395-6089; Fax: 626-564-9297; E-mail: dadougherty@caltech.edu.

[2] The abbreviations used are: nAChR, nicotinic acetylcholine receptor; *N*-Me, *N*-methyl; Cah, α-hydroxycysteine; Sah, α-hydroxyserine; Aah, α-hydroxyalanine; AChBP, acetylcholine-binding protein; NVOC, *o*-nitroveratryoxycarbonyl; NB, 2-nitrobenzyl; EtOAc, ethyl acetate.

EXPERIMENTAL PROCEDURES

Preparation of Cysteine Analogs—Cysteine analogs were prepared as 2-nitrobenzyl (NB) protected thiols. The 2-nitrobenzyl group was removed via irradiation with ~350-nm UV light prior to injection into *Xenopus* oocytes. A synthesis of nitroveratryl-protected cysteine, needed for control experiments, was described previously (25). Cyanomethyl esters of *N*-Me Cys and α-hydroxycysteine (Cah) were appended to the dinucleotide dCA, ligated to tRNA, and introduced to the nAChRs via unnatural amino acid mutagenesis as described previously (26).

Synthesis of N-Me-N-NVOC-Cys(SNB)-OCH$_2$CN—A 20-ml scintillation vial was loaded with 4 ml of methanol and placed over an ice water bath. To this was added 130 mg (5.7 mmol) of sodium. The mixture was stirred until the metal dissolved (~20 min). *N*-Me cysteine (370 mg, 2.7 mmol), prepared as described previously (27), was added to the vial, and the mixture was stirred for 10 min. 2-Nitrobenzyl bromide (520 mg, 2.6 mmol) was added in three portions to the stirring solution, turning a clear solution into a cloudy mixture containing a pale yellow precipitate. 1 h after the last addition, 20 ml of chilled ether was added. The precipitate was filtered, washed with 10 ml of chilled ether, and dried to afford *N*-Me-Cys(SNB)-OH as a crude, pale yellow solid. 100 mg (0.37 mmol) of this powder was used directly in the next step without further purification. The powder was suspended in 3 ml of water, and then an additional 1 ml of dioxane was added. Na_2CO_3 (59 mg, 0.56 mmol) was added, and the mixture was allowed to stir for 5 min prior to the addition of *o*-nitroveratryoxycarbonyl chloride (NVOC-chloride) (92 mg, 0.33 mmol) in 4 ml of dioxane. After stirring at room temperature for 48 h, the solution was diluted with 10 ml of CH_2Cl_2 and 10 ml of water. The organic layer was discarded, and the pH of the aqueous layer was decreased to 1 via the addition of 6 M HCl. Following extraction with CH_2Cl_2, the new organic layer was dried over Na_2SO_4 and poured over a silica plug. The plug was rinsed with 25 ml of EtOAc and then eluted with 2% AcOH in EtOAc. The yellow eluent was concentrated to reveal *N*-Me-*N*-NVOC-Cys(SNB)-OH as a pale yellow solid in 84% yield (158 mg, 0.310 mmol). R_f = 0.34 (2% AcOH in EtOAc); ^{1}H NMR (300 MHz, $CDCl_3$, 298 K) δ 7.89 (1H, m), 7.63 (1H, m), 7.47 (1H, t, J = 7.5 Hz), 7.36 (2H, m), 6.89 (1H, d, J = 14.1 Hz), 5.50 (2H, m), 4.68 (1H, m), 4.04 (2H, s), 3.86 (6H, s), 2.81–3.04 (5H, m); ^{13}C NMR (75 MHz, $CDCl_3$, 298K) δ 177.7, 174.9, 156.4, 153.7, 147.9, 139.3, 133.4, 133.2, 132.1, 128.6, 128.3, 125.6, 109.1, 108.1, 64.7, 58.9, 56.4, 56.4, 33.5, 32.3, 30.9; high-resolution MS analysis (FAB+) *m/z*: calculated 510.1182, found 510.1180.

N-Me-*N*-NVOC-Cys(SNB)-OH (58 mg, 0.11 mmol) was added to a 2-ml scintillation vial and suspended in 0.35 ml of chloroacetonitrile (5.5 mmol). Triethylamine (50 ml, 0.33 mmol) was added to the mixture, and the resulting solution was stirred for 4 h. The solution was diluted with 15 ml of water, and the organic layer was extracted with CH_2Cl_2 (×3), dried over Na_2SO_4, and concentrated to yield a yellow oil. The oil was purified by flash column chromatography on silica gel (50% EtOAC in hexanes) to afford *N*-Me, *N*-NVOC-Cys-(SNB)-OCH_2CN as a yellow oil in 62% yield (37 mg, 0.067 mmol). R_f = 0.25 (50% EtOAc in hexanes); ^{1}H NMR (300 MHz, $CDCl_3$, 298 K) δ 7.98 (1H, m), 7.70 (1H, m), 7.54 (1H, m), 7.43 (2H, m), 6.95 (1H, d, J = 14.1 Hz), 5.55 (2H, m), 4.72 (3H, m), 4.08 (2H, s), 4.00 (3H, s), 3.95 (3H, s), 2.89–3.10 (5H, m); ^{13}C NMR (75 MHz, $CDCl_3$, 298K) δ 168.5, 156.1, 153.7, 148.1, 133.3, 133.3, 133.2, 132.1, 128.7, 128.7, 127.9, 125.6, 109.5, 108.2, 64.9, 59.0, 56.4, 56.4, 49.1, 33.6, 32.7, 31.0; high-resolution MS analysis (FAB+) *m/z*: calculated 549.1291, found 549.1302.

Synthesis of HO-Cys(SNB)-OCH$_2$CN—The synthesis of 2-nitrobenzyl protected α-hydroxycysteine was based on a protocol reported by Kelly and co-workers (28). (2-Nitrophenyl)methanethiol (400 mg, 3.9 mmol) was prepared as described previously (29) and added to a flame-dried 50-ml, two-neck, round bottom flask equipped with a reflux condenser and under argon (g). To this was added methyl-(2*S*)-glycidate (660 mg, 3.9 mmol), triethylamine (0.54 ml, 3.9 mmol), and 20 ml of MeOH. The mixture was stirred for 5 h at reflux until completion of the reaction as determined by TLC. After cooling to room temperature, the mixture was concentrated *in vacuo*, and the resulting yellow oil was purified by flash column chromatography on silica gel (25% EtOAc in hexanes) to afford HO-Cys(SNB)-OMe in 35% yield (370 mg, 1.4 mmol). R_f = 0.44 (50% EtOAc in hexanes); ^{1}H NMR (300 MHz, $CDCl_3$, 298 K) δ 7.98 (1H, d, J = 8.2 Hz), 7.39–7.59 (3H, m), 4.44 (1H, b), 4.19 (2H, s), 3.79 (3H, s), 3.15 (1H, b), 2.89 (1H, dd, J = 14.4, 4.7 Hz), 2.75 (1H, dd, J = 14.4, 6.4 Hz); ^{13}C NMR (75 MHz, $CDCl_3$, 298K) δ 173.5, 148.6, 133.8, 133.0, 132.2, 128.3, 125.5, 71.2, 52.9, 35.3, 34.1; high-resolution MS analysis (FAB+) *m/z*: calculated 272.0593, found 272.0591.

HO-Cys(SNB)-OMe (44 mg, 1.6 mmol) was added to a 20-ml scintillation vial and dissolved in 10 ml of 1 M LiOH in 3:1:1 tetrahydrofuran:methanol:water. The mixture was stirred for 12 h at room temperature. The pH of the solution was adjusted to pH 12 via the addition of 2 M NaOH. The aqueous layer was washed with 30 ml of ether, and the organic layer was discarded. The pH of the aqueous layer was decreased to 1 via the addition of 6 M HCl and extracted with EtOAc. The new organic layer was washed with brine, dried over Na_2SO_4, and concentrated to yield HO-Cys(SNB)-OH as a yellow oil in 85% crude yield (350 mg, 1.4 mmol). Cyanomethyl esterification began with the addition of HO-Cys(SNB)-OH (250 mg, 0.97 mmol) to a 4-ml scintillation vial. Chloroacetonitrile (0.5 ml, 7.9 mmol) and triethylamine (0.40 ml, 2.9 mmol) were added to the vial, and the mixture was stirred for 12 h. The solution was diluted with 15 ml of water, and the organic layer was extracted with CH_2Cl_2 (×3), dried over Na_2SO_4, and concentrated to a yellow oil. The oil was purified by flash column chromatography on silica gel (50% EtOAC in hexanes) to afford HO-Cys(SNB)-OCH_2CN as a yellow oil in 55% yield (160 mg, 0.53 mmol). R_f = 0.35 (50% EtOAc in hexanes); ^{1}H NMR (400 MHz, $CDCl_3$, 298 K) δ 7.95 (1H, d), 7.39–7.57 (3H, m), 4.78 (2H, m), 4.52 (1H, m), 4.16 (2H, dd, J = 19.2, 13.3 Hz), 3.26 (1H, d, J = 5.5 Hz), 2.91 (1H, dd, J = 14.5, 3.9 Hz), 2.78 (1H, dd, J = 14.6, 5.9 Hz); ^{13}C NMR (100 MHz, $CDCl_3$, 298K) δ 171.4, 148.6, 133.4, 133.2, 132.2, 128.5, 125.5, 113.8, 71.0, 49.3, 35.1, 34.2; high-resolution MS analysis (FAB+) *m/z*: calculated 297.0545, found 297.0546.

Mutagenesis—Both conventional and unnatural mutagenesis were performed on mouse muscle embryonic nAChR ($\alpha1_2\beta1\gamma\delta$) cDNA in the pAMV vector using the standard Strat-

agene QuikChange protocol. For unnatural mutagenesis, a stop codon, TAG or TGA, was made at the site of interest and verified through sequencing. The β subunit contained a background mutation in the M2 transmembrane helix (βL9′S) that is known to lower whole-cell EC_{50} values (30, 31). The α1 subunit also contains a hemagglutinin epitope in the M3-M4 cytoplasmic loop. This epitope does not alter EC_{50} values in control experiments. cDNA was linearized with the restriction enzyme NotI. mRNA was prepared by *in vitro* transcription using the mMessage mMachine T7 kit (Ambion, Austin, TX).

Stage V-VI *Xenopus laevis* oocytes were injected with mRNA in a 2:1:1:1 or 10:1:1:1 ratio of α1:β1:γ:δ for conventional or unnatural amino acid mutagenesis experiments, respectively. Hydroxy or amino acids were appended to the dinucleotide dCA and enzymatically ligated to the truncated 74-nucleotide THG73 or TQOpS′ tRNA as described previously (26). NVOC and 2-nitrobenzyl protecting groups on the appended amino or α-hydroxy acids were removed by irradiation with UV light filtered to ~350 nm. For conventional experiments, 1–2 ng of mRNA was injected per oocyte in a single 75-nl injection. For unnatural amino acid experiments, each cell was injected with 75 nl of a 1:1 mixture of mRNA (20–25 ng of total mRNA) and tRNA (20–30 ng). Oocytes were incubated at 18 °C for 24–48 h after injection. Wild-type recovery experiments (injection of tRNA appended to the natural amino acid) were performed to evaluate the fidelity of the unnatural suppression experiments. Additional controls, injections of mRNA only and mRNA with 76-mer THG73 or TQOpS′, were also performed. Although currents were seen for 76-mer control experiments, EC_{50} and Hill values were distinct from the values obtained for 74-mer ligated to an α-hydroxy or amino acid. Conventional experiments with $\alpha4\beta2$ (32) and $\alpha4\beta4$ and $\alpha7$ (33) were performed as described previously.

Electrophysiology—The functional effects of mutation were evaluated using two-electrode voltage clamp electrophysiology. Electrophysiology experiments were performed 24–48 h after injection using the OpusXpress 6000A instrument (Axon Instruments) at a holding potential of −60 mV. A Ca^{2+}-free ND96 solution was used as the running buffer (96 mM NaCl, 2 mM KCl, 1 mM $MgCl_2$, and 5 mM HEPES, pH 7.5). Acetylcholine doses in Ca^{2+}-free ND96 were applied for 15 s followed by a 116-s wash with the running buffer. Dose-response data were obtained for ≥8 agonist concentrations on ≥7 cells. All EC_{50} and Hill coefficient values were obtained by fitting dose-response relations to the Hill equation and are reported as averages ± S.E. of the fit. A detailed error analysis of nonsense suppression experiments shows that data are reproducible to ±50% in EC_{50} (34).

Ab Initio Calculations—Structure building and subsequent *ab initio* calculations on CH_3CO-[Cys-Cys]-NH_2 were carried out using the Gaussian 03 software package (35) at the B3LYP/6–311++G(d,p) level of theory in the gas phase. The *cis* and *trans* isomers of a model peptide of the form CH_3CO-[Cys-Cys]-NH_2 with the S–S disulfide torsional angles of ±90 were constructed using the GausView molecule building tools. The geometric parameters for these starting structures were derived from the lowest energy conformers from previous *ab initio* calculations on a similar model peptide (21). Energy minimizations were performed on the four starting structures of the model peptide. The lowest energy structures from these model peptide calculations then served as scaffolds for constructing the initial ester and *N*-methyl structures, which were subsequently subject to energy minimization calculations. In total, the energies for 12 geometry-optimized structures were calculated, with four conformers for each model system. Further details are provided in Ref. 36. Calculations on simple cyclic amides and related structures were performed with SPARTAN (37).

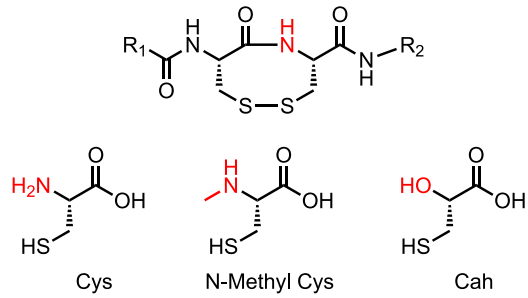

FIGURE 1. **Vicinal disulfide structure.** For model calculations of CH_3CO-[Cys-Cys]-NH_2, R_1 = CH_3 and R_2 = H. Also shown are the unnatural amino acids (*N*-Methyl Cys and Cah) used in this study.

RESULTS

Conformational Analysis and Experimental Design—As noted above, both the disulfide and the amide functionalities have two distinct conformations. In the computational studies described below, the gauche(+) and gauche(−) forms of the disulfide are very similar in energy and seem unlikely to play a strong discriminating role. Our work has emphasized the gauche(−) as this is the conformation seen in AChBP crystal structures.

For the amide unit, the issue is *cis-trans* isomerization. In a typical protein, a backbone amide shows a strong preference for the *trans* conformation (if proline is not involved). However, incorporation into an eight-membered ring is expected to favor the *cis* form. This expectation derives from studies of the conformational preferences of small molecules. For example, in cyclooctene, the *trans* form is substantially strained, and the *cis* form is preferred. *Ab initio* calculations we have performed show that an amide in an eight-membered alkane ring also shows a preference for *cis*; at the HF-6–31G** level of theory, *N*-methylacetamide shows a 2.5 kcal/mol preference for *trans*, whereas the cyclic amide shows a 5.4 kcal/mol preference for *cis*.

More sophisticated calculations at the B3LYP/6–311++G(d,p) level of theory on a model tripeptide (CH_3CO-[Cys-Cys]-NH_2, Fig. 1) for the nAChR vicinal disulfide likewise show an energetic preference for the *cis* amide, by 3.4 kcal/mol. This is not a large energy difference, and indeed, both *cis* and *trans* forms have been seen in crystal structures of molecules that contain a vicinal disulfide (38, 39). As such, it is reasonable to consider that perhaps *cis-trans* isomerization of the Cys-192-Cys-193 backbone may play a role in gating of nAChRs (10, 18, 19, 21, 22). This structural change could then easily be imagined to propagate along the protein backbone and perhaps initiate the "conformational wave" (40) that leads to gating.

To test this model, we sought modifications to the vicinal disulfide that would alter the innate *cis-trans* bias of the system.

TABLE 1
EC_{50}, Hill coefficient (± S.E.), and $\Delta G°$ values for mutations made to $\alpha 1_2\beta 1\gamma\delta$

Mutation	EC_{50}	Hill	$\Delta G°$
	μM		*kcal/mol*
$\alpha 1\beta 1\gamma\delta$	18 ± 0.2	1.4 ± 0.01	
$\alpha 1$(C192A)$\beta 1\gamma\delta$	660 ± 20	1.3 ± 0.05	2.1
$\alpha 1$(C192S)$\beta 1\gamma\delta$	520 ± 20	1.5 ± 0.08	2.0
$\alpha 1$(C193A)$\beta 1\gamma\delta$	140 ± 3	1.2 ± 0.02	1.2
$\alpha 1$(C193S)$\beta 1\gamma\delta$	150 ± 7	1.4 ± 0.07	1.3
$\alpha 1\beta$(L9′S)$\gamma\delta$	0.61 ± 0.04	1.4 ± 0.1	
$\alpha 1$(S191A)$\beta 1$(L9′S)$\gamma\delta$	0.31 ± 0.02	1.1 ± 0.05	
$\alpha 1$(S191A/C193A)$\beta 1$(L9′S)$\gamma\delta$	5.2 ± 0.4	1.0 ± 0.07	1.7
$\alpha 1$(S191A/C193S)$\beta 1$(L9′S)$\gamma\delta$	9.5 ± 0.7	0.96 ± 0.06	2.0
$\alpha 1$(S191A/C193Cah)$\beta 1$(L9′S)$\gamma\delta$	49 ± 4	0.80 ± 0.03	3.0
$\alpha 1$(S191A/C193(*N*-methyl Cys))$\beta 1$(L9′S)$\gamma\delta$	39 ± 2	0.88 ± 0.04	2.9
$\alpha 1$(S191Aah)$\beta 1$(L9′S)$\gamma\delta$	31 ± 3	1.1 ± 0.09	2.7
$\alpha 1$(S191A)$\beta 1$(L9′S)γ(D174N)δ(D180N)	160 ± 7	1.3 ± 0.06	3.7

For example, it is well known (41) that esters have a stronger *trans* preference than amides; methyl acetate prefers *trans* by 8.0 kcal/mol when compared with the 2.5 kcal/mol noted for *N*-methylacetamide above. It is also well established that *N*-methylation reduces the innate *trans* preference of a backbone amide in peptides and proteins (42, 43). Thus, we considered the strategy of modifying the amide linkage of the vicinal disulfide. If *cis-trans* isomerization of this unit plays a role in receptor function, then the ester and *N*-methyl modifications should have opposite effects.

To test this prediction *in silico*, we performed comparable B3LYP/6–311++G(d,p) calculations on the ester and *N*-methyl amide analogs of the vicinal disulfide model discussed above. The results are consistent with expectations based on the conformational preferences of small molecules discussed above. When compared with the natural backbone (an amide), which favors the *cis* by 3.4 kcal/mol, the ester favors the *trans* by 1.4 kcal/mol. *N*-Methylation increases the *cis* preference of the parent (the amide backbone) to 9.3 kcal/mol, consistent with experimental studies on a similar system reported by Hondal and co-workers (22).

It is difficult to apply these data to nAChR function in a quantitative way; calculations were performed on model tripeptides and depsipeptides in the gas phase, not on an ~2.5-MDa pentameric, polytropic receptor protein in a cell membrane. However, the predictions of the calculations are clear. If *cis-trans* isomerization of the vicinal disulfide amide is functionally important, the two modifications considered, backbone ester incorporation and amide *N*-methylation, should have opposite effects on receptor function.

Both modifications can be site-specifically introduced into the nAChR using the *in vivo* nonsense suppression methodology that has been developed in our laboratories over the past 20 years (44, 45). We thus set out to prepare and characterize the appropriate mutant receptors as a test of the computational modeling.

Mutagenesis Studies—Initial control experiments involving the vicinal disulfide clarified the effect of eliminating this structure. We found that we could introduce Ala or Ser at Cys-192 or Cys-193 of the wild-type muscle subtype receptor and obtain functional receptors. The EC_{50} value shifts ~8–40-fold (Table 1), and current sizes comparable with those for the wild-type receptor are seen. We repeated these studies in three other subtypes of the nAChR, the neuronal receptors $\alpha 4\beta 2$, $\alpha 4\beta 4$, and $\alpha 7$, and saw similar effects but with generally larger shifts in EC_{50} (~20–200-fold, supplemental Table S1).

In 1985, Mishina *et al.* (17) reported that C192S and C193S mutants of *Torpedo* nAChR, a close paralog of the muscle nAChR, were unresponsive to high concentrations of ACh but did bind α-bungarotoxin. These findings suggested that mutation of either residue results in a receptor that is properly folded but does not function. However, our present finding that the nAChR can be activated even in the presence of mutated 192 and 193 side chains indicates that the vicinal disulfide linkage increases the efficiency of receptor function but is not absolutely required.

In these studies, we are reporting EC_{50} values, a functional measure that includes contributions from both ligand binding and receptor gating. For the residues emphasized here, there is no evidence that Cys-192 and Cys-193 interact strongly and directly with agonists, and so we anticipate that mutations primarily impact receptor gating, although we cannot prove that unambiguously. In the upcoming discussion, we will be describing the results of mutant cycle analysis studies. It is standard practice in that field to convert coupling interactions (nonadditivity) to free energies ($\Delta\Delta G°$) (46, 47). In view of this, and solely for the purpose of discussion, we will put all changes in EC_{50} values on a similar energy scale: $\Delta G° = RT\ln(EC_{50}(\text{mutant})/EC_{50}(\text{wild type}))$.

Before launching detailed nonsense suppression experiments with *N*-methyl Cys and Cah (cysteine, α-hydroxy) we considered several conditions and nAChR subtypes, including the muscle receptor $\alpha 1_2\beta 1\gamma\delta$ and the neuronal subtypes $\alpha 4\beta 2$, $\alpha 4\beta 4$, and $\alpha 7$. We chose to focus on the muscle subtype for the following reasons. The muscle subtype is, in general, the most studied nAChR, and it is also the receptor that gave the highest currents for nonsense suppression experiments with *N*-methyl Cys and Cah. In addition, it has a defined stoichiometry, a substantial advantage over the $\alpha 4\beta 2$ and $\alpha 4\beta 4$ receptors (which each have two possible subunit stoichiometries). It also required considerably lower agonist concentrations than those needed for experiments with $\alpha 7$.

For our nonsense suppression experiments in $\alpha 1_2\beta 1\gamma\delta$, we used the well documented leucine-to-serine mutation at the 9′ position in the M2 region of nAChR. This mutation renders the nAChR ~40 times more sensitive to agonists, as judged by the decrease in EC_{50} (30, 31). The 9′ position lies some 60 Å from the agonist binding site and from the vicinal disulfide studied

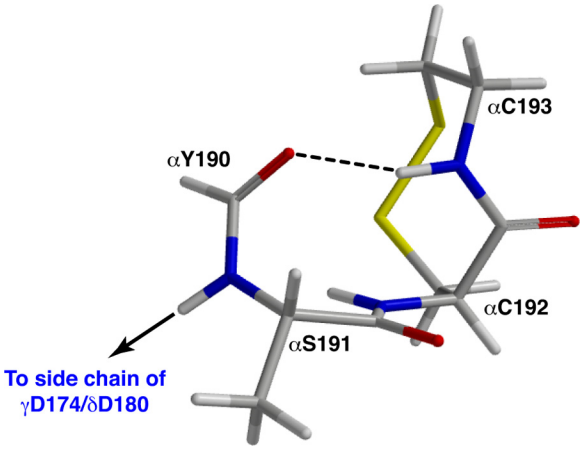

FIGURE 2. **The β turn found in AChBP structures.** The structure is from Protein Data Bank (PDB) file 1UV6 (24) and was modified to contain an Ala at Ser-191.(24) The side chain of Tyr-190 is truncated (replaced with a hydrogen) for simplicity.

here, and therefore it does not directly affect the Cys-192-Cys-193 region but instead affects receptor gating. This change favors the open state of the channel once an agonist molecule has bound, also increasing the efficacy of some agonists.

We also introduced a mutation in the α1 subunit, S191A, of all mutant proteins used in double mutant cycle analyses as this mutant promoted more reliable current sizes for nonsense suppression experiments with α-hydroxy acids at position 191, experiments that will be discussed in greater detail below. We showed previously (48) that the S191A mutation has a minor effect on receptor function (see also Table 1) and that the incorporation of Aah (α-hydroxyalanine) or Sah (α-hydroxyserine) at Ser-191 results in the same EC_{50} shift.

In the crucial experiments involving alteration of the backbone of the Cys-192-Cys-192 unit, we find that replacement of Cys-193, whose backbone is within the eight-membered ring formed by the vicinal disulfide, with either *N*-methyl Cys or Cah produces *similar* results. Both mutations are loss-of-function, and their impacts are comparable in magnitude, with a ΔG° value of ~3 kcal/mol. These are relatively large effects for such subtle mutations (larger than the Cys-to-Ala mutations), suggesting an important functional role for the backbone of Cys-193. These results are not consistent with a functional role for *cis-trans* isomerization, which predicts opposite effects for the two modifications.

Although differing in their anticipated impact on *cis-trans* isomerization, the two backbone mutations are similar in another regard; both ablate the hydrogen bond-donating ability associated with the NH of the parent amide. An inspection of AChBP structures reveals a potential acceptor for such a hydrogen bond donor: the carbonyl of residue Tyr-190, a conserved member of the agonist binding site. This hydrogen bond is generally present in AChBP structures, and it defines a distorted Type I β turn, with Tyr-190, Ser-191, Cys-192, and Cys-193 being residues *i* to *i*+3, respectively (Fig. 2).

The inclusion of Ser-191 in the β turn suggested a more complex interaction than just a simple hydrogen bond. Previous work from our laboratories (48) strongly supported a model in which the backbone NH of Ser-191 makes an *intersubunit* hydrogen bond to the side chain of a critical Asp in the γ/δ subunits (γAsp-174/δAsp-180). This hydrogen bond contributes to ion channel gating. In that study, we removed the critical NH by preparing the mutant S191Sah or S191Aah, producing one of the largest perturbations ever observed in our laboratories for the introduction of a backbone ester. A double mutant cycle analysis combining S191Sah and γD174N/δD180N provided strong functional evidence for an interaction, with a coupling energy $\Delta\Delta G^\circ = 2.7$ kcal/mol. However, many studies have shown that a backbone ester mutation not only removes a backbone NH that can donate a hydrogen bond, it also weakens the hydrogen bond-accepting ability of the associated *i-1* carbonyl (49–54). For Ser-191, the *i-1* carbonyl comes from Tyr-190, the carbonyl implicated in the hydrogen bond of the β turn discussed above. Could the S191Sah effect be so large because it both deletes the hydrogen bond to γAsp-174/δAsp-180 and weakens an important β turn hydrogen bond?

We have now found support for the β turn hydrogen bond. A mutant cycle analysis (Fig. 3*A*) combining S191Aah and C193(*N*-methyl Cys) shows a strong coupling energy, with $\Delta\Delta G^\circ = 2.7$ kcal/mol (Table 2). This finding supports the existence of a novel, 3-residue, hydrogen bond network, in which the NH of Cys-193 hydrogen bonds to the carbonyl of the peptide bond between Tyr-190 and Ser-191. In addition, the NH of the Tyr-190-Ser-191 peptide bond hydrogen-bonds to the side chain of γAsp-174/δAsp-180 (Fig. 3).

If this hydrogen-bonding network exists, energetic coupling between the NH of Cys-193 and the side chain of γAsp-174/δAsp-180 is expected. Indeed, we find strong coupling energies between the γD174N/δD180N mutation and either C193(*N*-methyl Cys) or C193Cah, with $\Delta\Delta G^\circ$ values of 2.0 and 2.2 kcal/mol (Table 2, Fig. 3*B*). The magnitude of this interaction is quite significant when one considers the linkage is from a residue in the α subunit, through a second residue in the α subunit, and then across the subunit interface to a residue in the γ/δ subunit.

These results suggest a key role for the peptide bond of the Cys-192-Cys-193 unit. In support of this view, mutations that remove the disulfide but keep the peptide bond are much less impactful. Mutant cycles that link C193A to the backbone NH of Ser-191 or to γD174N/δD180N produce $\Delta\Delta G^\circ$ coupling energies of 0.99 and 0.80 kcal/mol, respectively, clearly smaller than seen with backbone mutations.

DISCUSSION

The present work began as an effort to evaluate a possible role for *cis-trans* isomerization of the Cys-192-Cys-193 peptide bond embedded in the unusual vicinal disulfide of the α subunits of nAChRs. Our data do not support such a transition, but instead reveal an extended network of hydrogen bonds that appears to play a significant role in receptor function. In this network, the backbone NH of Cys-193 hydrogen-bonds to the backbone carbonyl of Tyr-190. The Tyr-190 carbonyl is, in turn, connected to the NH of Ser-191, which hydrogen-bonds across the subunit interface to the side chain of γAsp-174/δAsp-180. The model is strongly supported by long-range double mutant cycle analysis that links the γD174N/δD180N mutation to Cys-193 backbone mutations. Removing the NH of Cys-

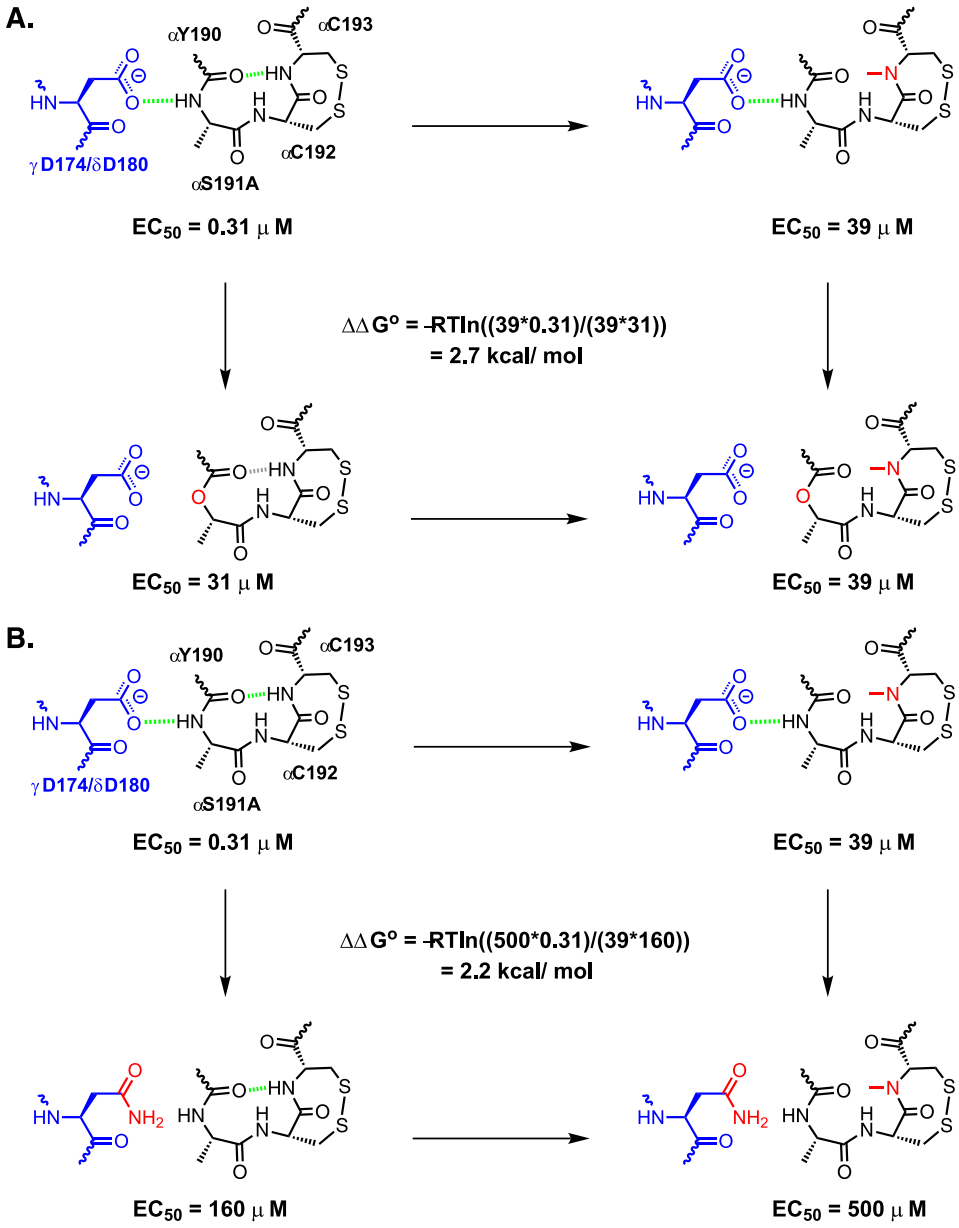

FIGURE 3. **Double mutant cycle analysis.** *A*, coupling between backbone mutations at αSer-191 and αCys-193. Note that introduction of the α-hydroxy acid at Ser-191 attenuates the hydrogen bond acceptor for the hydrogen bond with Cys-193 and removes the hydrogen bond donor for the hydrogen bond to γAsp-174/δAsp-180. *B*, long-range coupling between a backbone mutation at αSer-191 and a side chain mutation at γAsp-174/δAsp-180.

TABLE 2
EC_{50}, Hill coefficient (± S.E.), and $\Delta\Delta G°$ values for double mutations made to $\alpha1_2\beta1\gamma\delta$

Double mutation	EC_{50}	Hill	$\Delta\Delta G°$
	μM		*kcal/mol*
α1(S191Aah/C193A)β1(L9′S)γδ	97 ± 10	0.76 ± 0.04	0.99
α1(S191Aah/C193S)β1(L9′S)γδ	100 ± 7	0.93 ± 0.05	1.3
α1(S191Aah/C193(*N*-methyl Cys))β1(L9′S)γδ	39 ± 4	0.70 ± 0.03	2.7
α1(S191Aah)β1(L9′S)γ(D174N)δ(D180N)	140 ± 10	1.7 ± 0.2	2.8
α1(S191A/C193A)β1(L9′S)γ(D174N)δ(D180N)	600 ± 20	1.5 ± 0.07	0.8
α1(S191A/C193S)β1(L9′S)γ(D174N)δ(D180N)	780 ± 20	1.6 ± 0.06	1.1
α1(S191A/C193Cah)β1(L9′S)γ(D174N)δ(D180N)	800 ± 40	1.5 ± 0.05	2
α1(S191A/C193(*N*-methyl Cys))β1(L9′S)γ(D174N)δ(D180N)	500 ± 20	1.5 ± 0.07	2.2

193 either by ester incorporation or by *N*-methylation produces the same effect: a coupling energy $\Delta\Delta G°$ of 2.0–2.2 kcal/mol to the Asp-to-Asn mutations.

The β turn hydrogen bond between the carbonyl of Tyr-190 and the NH of Cys-193 was suggested by AChBP structures (23, 24). Note, however, that the second hydrogen bond of the triad, that between the NH of Ser-191 and the side chain of γAsp-174/δAsp-180, is not present in AChBPs and represents a significant difference between the actual nAChRs and the model AChBP systems. In fact, in crystal structures of AChBP, the

loop F residue that corresponds to γAsp-174/δAsp-180 is far from the C loop of the adjacent subunit, and in the cryoelectron microscopy structures of *Torpedo* nAChR, the residue is over 15 Å from the C loop (55, 56).

Given these data, what then is the functional role of the Cys-192-Cys-193 vicinal disulfide of nAChR α subunits? Here we present a speculative model. An early mutagenesis study of the *Torpedo* nAChR indicated that both the C192S and the C193S mutants were unresponsive to high concentrations of ACh (17). However, DTT reduction of the vicinal disulfide produced only partial diminution of receptor function (6), and alkylation of one of these cysteines by bromoacetylcholine (8) or QBr (16) reinstates partial function despite the absence of the vicinal disulfide. Here we also find that in mouse muscle and several neuronal nAChRs, conventional mutations at Cys-192/Cys-193, although certainly loss-of-function, do produce functional receptors. In the present case, C192A and C193A are both loss-of-function, but the magnitudes of the effects (2.0 and 1.7 kcal/mol with the α1S191A background mutation) are *less* than seen with the backbone mutations (2.9 and 3.0 kcal/mol), for which the disulfide linkage is intact.

We propose that the role of the vicinal disulfide is to shape the structure of the β turn between Tyr-190 and Cys-193. The resultant distorted β turn may then help position the backbone NH of Ser-191 for formation of the second hydrogen bond. Such a model is supported by the observation that backbone mutations at Cys-193 are strongly loss-of-function, suggesting that backbone positioning in this β turn is critical for receptor function.

We noted above that the β turn seen in AChBP structures is substantially distorted from idealized dihedral angle values for a Type I β turn. Quantum mechanical calculations (see details in the supplemental material) establish that reducing the disulfide does indeed allow the β turn to relax toward a more typical geometry. This structural change impacts the energetic strength of the β turn hydrogen bond only modestly (0.3–0.4 kcal/mol), but it does alter the positioning of the peptide linkage between Tyr-190 and Ser-191. Thus, we propose that the essential consequence of the distortion of the β turn induced by the disulfide is not the energetic weakening of the β turn hydrogen bond, but rather the positioning of Ser-191 in an orientation that is favorable for interaction with γAsp-174/δAsp-180.

Our gating model is thus as follows. In the closed state of the receptor, the β turn hydrogen bond is formed, but the intersubunit hydrogen bond (Ser-191 to γAsp-174/δAsp-180) is not (consistent with the AChBP crystal structures). The β turn hydrogen bond is essential to proper formation of the agonist binding site (recall that Tyr-190 is residue C1 of the highly conserved cluster of aromatic amino acids that delineate the agonist binding site). Activation involves formation of the intersubunit hydrogen bond, an event that is facilitated by proper positioning of the backbone NH of Ser-191 by the vicinal disulfide and the β turn hydrogen bond. The two hydrogen bonds should be mutually reinforcing, making the amide a stronger hydrogen bond acceptor and donor, and so in our model, the driving force for movement of the F loop (containing γAsp-174/δAsp-180) is the formation of a network of hydrogen bonds. As discussed elsewhere (48), this structural change at the subunit interface then contributes to an early phase of the conformational wave of receptor gating.

Note that our conventional mutations of Cys-192 and Cys-193, both of which are loss-of-function, are consistent with this model. The C192A and C193A mutants remove the disulfide and allow the β turn to relax to a more typical conformation (mirrored in the calculations). With the β turn relaxed, the backbone NH of Ser-191 is not positioned optimally to form a hydrogen bond with γAsp-174/δAsp-180, resulting in a loss of receptor function. The critical role of the peptide bond is further supported by our observation that disruption of the vicinal disulfide (C193A) perturbs the hydrogen bond network in a much more subtle manner than removal of the hydrogen bond donor of Cys-193. Other Cys-loop receptors lack the vicinal disulfide of the nAChR α subunit, and it will be interesting to see whether the β turn and intersubunit hydrogen bond survive in a different environment.

The vicinal disulfide has a unique historical connection to γAsp-174/δAsp-180. Czajkowski *et al.* (11, 12, 14, 57) linked the reduced cysteine side chain at position α193 to γAsp-174/δAsp-180 with a 9 Å cross-linker. Mutation of the aspartate resulted in a large loss of receptor function, leading to the suggestion that the negative charge of the aspartate side chain interacts directly with the positive charge of the agonist. Subsequent mutagenesis studies showed that the positive charge of agonists makes a cation-π interaction to a conserved tryptophan (32, 58) and not a direct interaction with the aspartate. Crystallographic studies of AChBP supported the cation-π interaction and revealed that γAsp-174/δAsp-180 is positioned far from the agonist binding site (24). Single channel studies from the early 2000s suggested that the residue was important for channel gating (and not binding) (59, 60); however, a role for the aspartate was only recently discovered. In 2008, we reported that γAsp-174/δAsp-180 is a member of an important intersubunit hydrogen bond linking the F and C loops and contributing to channel gating (48). We now report an additional, larger group of hydrogen bonds once again linking the vicinal disulfide to this important residue.

In summary, our mutagenesis studies unambiguously establish, through mutant cycle analysis, a hydrogen-bonding network, beginning at the backbone NH of the Cys-192-Cys-193 disulfide, through the backbone amide linkage between Tyr-190-Ser-191, and across the subunit interface to the side chain of γAsp-174/δAsp-180. Based on this, we present a speculative model in which the transition of the receptor from the closed to the open state involves formation of a network of tandem hydrogen bonds. In this model, the vicinal disulfide of the α subunit distorts the C loop β-turn to better position the backbone NH of Ser-191 for optimal formation of an intersubunit hydrogen bond.

REFERENCES

1. Corringer, P. J., Le Novère, N., and Changeux, J. P. (2000) *Annu. Rev. Pharmacol. Toxicol.* **40,** 431–458
2. Grutter, T., and Changeux, J. P. (2001) *Trends Biochem. Sci.* **26,** 459–463
3. Karlin, A. (2002) *Nat. Rev. Neurosci.* **3,** 102–114
4. Jensen, A. A., Frølund, B., Liljefors, T., and Krogsgaard-Larsen, P. (2005) *J. Med. Chem.* **48,** 4705–4745
5. Romanelli, M. N., Gratteri, P., Guandalini, L., Martini, E., Bonaccini, C.,

and Gualtieri, F. (2007) *ChemMedChem* **2,** 746–767
6. Karlin, A., and Bartels, E. (1966) *Biochim. Biophys. Acta* **126,** 525–535
7. Karlin, A. (1969) *J. Gen. Physiol.* **54,** 245–264
8. Silman, I., and Karlin, A. (1969) *Science* **164,** 1420–1421
9. Kao, P. N., Dwork, A. J., Kaldany, R. R., Silver, M. L., Wideman, J., Stein, S., and Karlin, A. (1984) *J. Biol. Chem.* **259,** 11662–11665
10. Kao, P. N., and Karlin, A. (1986) *J. Biol. Chem.* **261,** 8085–8088
11. Czajkowski, C., and Karlin, A. (1991) *J. Biol. Chem.* **266,** 22603–22612
12. Czajkowski, C., Kaufmann, C., and Karlin, A. (1993) *Proc. Natl. Acad. Sci. U.S.A.* **90,** 6285–6289
13. Damle, V. N., and Karlin, A. (1980) *Biochemistry* **19,** 3924–3932
14. Martin, M., Czajkowski, C., and Karlin, A. (1996) *J. Biol. Chem.* **271,** 13497–13503
15. Walker, J. W., Lukas, R. J., and McNamee, M. G. (1981) *Biochemistry* **20,** 2191–2199
16. Chabala, L. D., and Lester, H. A. (1986) *J. Physiol.* **379,** 83–108
17. Mishina, M., Tobimatsu, T., Imoto, K., Tanaka, K., Fujita, Y., Fukuda, K., Kurasaki, M., Takahashi, H., Morimoto, Y., Hirose, T., Inayama, S., Takahashi, T., Kuno, M., and Numa, S. (1985) *Nature* **313,** 364–369
18. Avizonis, D. Z., Farr-Jones, S., Kosen, P. A., and Basus, V. J. (1996) *J. Am. Chem. Soc.* **118,** 13031–13039
19. Creighton, C. J., Reynolds, C. H., Lee, D. H., Leo, G. C., and Reitz, A. B. (2001) *J. Am. Chem. Soc.* **123,** 12664–12669
20. Gao, F., Mer, G., Tonelli, M., Hansen, S. B., Burghardt, T. P., Taylor, P., and Sine, S. M. (2006) *Mol. Pharmacol.* **70,** 1230–1235
21. Hudáky, I., Gáspári, Z., Carugo, O., Cemazar, M., Pongor, S., and Perczel, A. (2004) *Proteins* **55,** 152–168
22. Ruggles, E. L., Deker, P. B., and Hondal, R. J. (2009) *Tetrahedron* **65,** 1257–1267
23. Brejc, K., van Dijk, W. J., Klaassen, R. V., Schuurmans, M., van Der Oost, J., Smit, A. B., and Sixma, T. K. (2001) *Nature* **411,** 269–276
24. Celie, P. H., van Rossum-Fikkert, S. E., van Dijk, W. J., Brejc, K., Smit, A. B., and Sixma, T. K. (2004) *Neuron* **41,** 907–914
25. Silverman, S. K. (1998). *I. Conformational and Charge Effects on High-spin Organic Polyradicals. II Studies on the Chemical-scale Origin of Ion Selectivity in Potassium Channels*. Ph.D. thesis, California Institute of Technology, Pasadena, CA
26. Nowak, M. W., Gallivan, J. P., Silverman, S. K., Labarca, C. G., Dougherty, D. A., and Lester, H. A. (1998) *Methods Enzymol.* **293,** 504–529
27. Park, J. D., and Kim, D. H. (2002) *J. Med. Chem.* **45,** 911–918
28. Deechongkit, S., You, S. L., and Kelly, J. W. (2004) *Org. Lett.* **6,** 497–500
29. Sohn, C. H., Chung, C. K., Yin, S., Ramachandran, P., Loo, J. A., and Beauchamp, J. L. (2009) *J. Am. Chem. Soc.* **131,** 5444–5459
30. Filatov, G. N., and White, M. M. (1995) *Mol Pharmacol* **48,** 379–384
31. Labarca, C., Nowak, M. W., Zhang, H., Tang, L., Deshpande, P., and Lester, H. A. (1995) *Nature* **376,** 514–516
32. Xiu, X., Puskar, N. L., Shanata, J. A., Lester, H. A., and Dougherty, D. A. (2009) *Nature* **458,** 534–537
33. Puskar, N. L., Xiu, X., Lester, H. A., and Dougherty, D. A. (2011) *J. Biol. Chem.* **286,** 14618–14627
34. Torrice, M. M. (2009) *Chemical-scale Studies of the Nicotinic And Muscarinic Acetylcholine Receptors*. Ph.D. thesis, California Institute of Technology, Pasadena, CA
35. Frisch, M. J., Trucks, G. W., Schlegel, H. B., Scuseria, G. E., Robb, M. A., Cheeseman, J. R., Montgomery, J. A., Vreven, T., Kudin, K. N., Burant, J. C., Millam, J. M., Iyengar, S. S., Tomasi, J., Barone, V., Mennucci, B., Cossi, M., Scalmani, G., Rega, N., Petersson, G. A., Nakatsuji, H., Hada, M., Ehara, M., Toyota, K., Fukuda, R., Hasegawa, J., Ishida, M., Nakajima, T., Honda, Y., Kitao, O., Nakai, H., Klene, M., Li, X., Knox, J. E., Hratchian, H. P., Cross, J. B., Bakken, V., Adamo, C., Jaramillo, J., Gomperts, R., Stratmann, R. E., Yazyev, O., Austin, A. J., Cammi, R., Pomelli, C., Ochterski, J. W., Ayala, P. Y., Morokuma, K., Voth, G. A., Salvador, P., Dannenberg, J. J., Zakrzewski, V. G., Dapprich, S., Daniels, A. D., Strain, M. C., Farkas, O., Malick, D. K., Rabuck, A. D., Raghavachari, K., Foresman, J. B., Ortiz, J. V., Cui, Q., Baboul, A. G., Clifford, S., Cioslowski, J., Stefanov, B. B., Liu, G., Liashenko, A., Piskorz, P., Komaromi, I., Martin, R. L., Fox, D. J., Keith, T., Laham, A., Peng, C. Y., Nanayakkara, A., Challacombe, M., Gill, P. M. W., Johnson, B., Chen, W., Wong, M. W., Gonzalez, C., and Pople, J. A. (2004) *Gaussian 03*, Revision C.02, Gaussian, Inc., Wallingford, CT
36. Gleitsman, K. R. (2010). *Chemical-scale Studies of the Nicotinic Acetylcholine Receptor: Insights from Amide-to-Ester Backbone Mutagenesis*. Ph.D. thesis, California Institute of Technology, Pasadena, CA
37. *SPARTAN*, Wavefunction, Inc., Irvine, CA
38. Capasso, S., Mattia, C., Mazzarella, L., and Puliti, R. (1977) *Acta Crystallogr. B Struct. Commun.* **33,** 2080–2083
39. Hata, Y., Matsuura, Y., Tanaka, N., Ashida, T., and Kakudo, M. (1977) *Acta Crystallogr. B Struct. Commun.* **33,** 3561–3564
40. Grosman, C., Zhou, M., and Auerbach, A. (2000) *Nature* **403,** 773–776
41. Dugave, C., and Demange, L. (2003) *Chem. Rev.* **103,** 2475–2532
42. Aubry, A., Vitoux, B., Boussard, G., and Marraud, M. (1981) *Int. J. Pept. Protein Res.* **18,** 195–202
43. Vitoux, B., Aubry, A., Cung, M. T., Boussard, G., and Marraud, M. (1981) *Int. J. Pept. Protein Res.* **17,** 469–479
44. Beene, D. L., Dougherty, D. A., and Lester, H. A. (2003) *Curr. Opin. Neurobiol.* **13,** 264–270
45. Nowak, M. W., Kearney, P. C., Sampson, J. R., Saks, M. E., Labarca, C. G., Silverman, S. K., Zhong, W., Thorson, J., Abelson, J. N., Davidson, N., Schultz, P. G., Dougherty, D. A., and Lester, H. A. (1995) *Science* **268,** 439–442
46. Horovitz, A. (1996) *Fold. Des.* **1,** R121–R126
47. Makhatadze, G. I., Loladze, V. V., Ermolenko, D. N., Chen, X., and Thomas, S. T. (2003) *J. Mol. Biol.* **327,** 1135–1148
48. Gleitsman, K. R., Kedrowski, S. M., Lester, H. A., and Dougherty, D. A. (2008) *J. Biol. Chem.* **283,** 35638–35643
49. Beligere, G. S., and Dawson, P. E. (2000) *J. Am. Chem. Soc.* **122,** 12079–12082
50. Blankenship, J. W., Balambika, R., and Dawson, P. E. (2002) *Biochemistry* **41,** 15676–15684
51. Deechongkit, S., Dawson, P. E., and Kelly, J. W. (2004) *J. Am. Chem. Soc.* **126,** 16762–16771
52. Deechongkit, S., Nguyen, H., Powers, E. T., Dawson, P. E., Gruebele, M., and Kelly, J. W. (2004) *Nature* **430,** 101–105
53. Koh, J. T., Cornish, V. W., and Schultz, P. G. (1997) *Biochemistry* **36,** 11314–11322
54. Nakhle, B. M., Silinski, P., and Fitzgerald, M. C. (2000) *J. Am. Chem. Soc.* **122,** 8105–8111
55. Miyazawa, A., Fujiyoshi, Y., Stowell, M., and Unwin, N. (1999) *J. Mol. Biol.* **288,** 765–786
56. Unwin, N. (2005) *J. Mol. Biol.* **346,** 967–989
57. Czajkowski, C., and Karlin, A. (1995) *J. Biol. Chem.* **270,** 3160–3164
58. Zhong, W., Gallivan, J. P., Zhang, Y., Li, L., Lester, H. A., and Dougherty, D. A. (1998) *Proc. Natl. Acad. Sci. U.S.A.* **95,** 12088–12093
59. Akk, G., Zhou, M., and Auerbach, A. (1999) *Biophys. J.* **76,** 207–218
60. Sine, S. M., Shen, X. M., Wang, H. L., Ohno, K., Lee, W. Y., Tsujino, A., Brengmann, J., Bren, N., Vajsar, J., and Engel, A. G. (2002) *J. Gen. Physiol.* **120,** 483–496